Numerical analysis of ballistic imaging for revealing liquid breakup in dense sprays

D. L. Sedarsky *, E. Berrocal
Department of Physics, Lund University, Lund, Sweden
M. A. Linne
Department of Applied Mechanics, Chalmers University, Gothenburg, Sweden

Abstract

This work demonstrates the capacity of a Ballistic Imaging (BI) instrument to suppress diffuse photons and improve image contrast, making it possible to view fluid structure in a spray where a fog of droplets occludes the near-field. Analysis of the system is performed by means of a numerical system model. The model simulates light propagation and scattering in the measurement volume using a Monte Carlo based solution to the radiative transfer equation, and includes treatment of the full system optics using a custom ray-tracing code. Simulation results for the validation case where source light illuminates a test chart inside a turbid (optical depth = 14) solution of monodisperse polystyrene spheres (d = 0.7 μm) show good agreement with experimental images. The model is further applied by replacing the solution of polystyrene spheres with a spray-like scattering medium. Here, we investigate the temporal characteristics of an ultrashort (100 fs) laser signal crossing a volume containing a polydisperse distribution of fuel droplets with a representative Sauter mean diameter, d_{32} = 23 μm. These quantitative predictions allow the effectiveness of both the spatial and temporal filtering of the BI instrument to be estimated. Results from the model demonstrate that the spatial filtering and time gating effects of the BI system significantly improve image contrast, revealing information that is not available with conventional imaging techniques.

Introduction

At present, laser diagnostics of dense multiphase flow fields are greatly restricted due to inherent difficulties imposed by signal attenuation and multiple-scattering noise. The near-nozzle region of an atomizing liquid-fuel injection spray is one important example. In order to characterize and fully understand multiphase flows, reliable, affordable, non-intrusive measurements of dense region flow structure must be developed. Ballistic imaging (BI) is an extension of shadowgraphy that utilizes visible light for detailed quantitative measurements in optically dense systems. BI diagnostics pertaining to spray and combustion applications were reviewed by Linne, *et al.* in 2009 [1]. BI applications mitigate distortion from multiply-scattered light by carefully selecting the photons collected to form a shadowgram image, as shown in Figure 1. This can be accomplished using discrimination methods that make use of the properties of the transmitted light. For example, propagation direction, exit time, polarization, and coherence properties can all be used for segregation. Most photons traversing an optically thick measurement volume are scattered multiple times (diffuse photons), distorting the image information they represent. Some photons scatter only marginally (snake photons), and thus, traverse the medium with some degree of information. Finally, some photons pass without scattering (ballistic photons) preserving the exact profile of the incident laser light. From the appropriate selection of both snake and ballistic photons, high-resolution shadowgram images can be formed even in dense conditions. In order to improve BI results for a specific spray measurement, it is essential to understand the composite effects of the light source, the turbid measurement volume and the detection optics. Due to the successive scattering interactions, such as multiple scattering within the turbid medium and reflection/refraction through the collection optics, the temporal and spatial shape of the resulting signal is often counter-intuitive. Hence, a system model is required in order to properly understand the properties of the signal and effectively optimize the BI measurement.

The scattering of light within a turbid medium, such as a spray, can be loosely classified into 3 regimes based on the optical thickness of the medium:

– In the *single scattering regime* the average number of scattering events ≤ 1 and the non-scattered (ballistic) photons are dominant. For off-axis detection, the single scattering approximation which assumes that photons have experienced only one scattering event prior arriving to the detector applies.

*Corresponding author: david.sedarsky@forbrf.lth.se

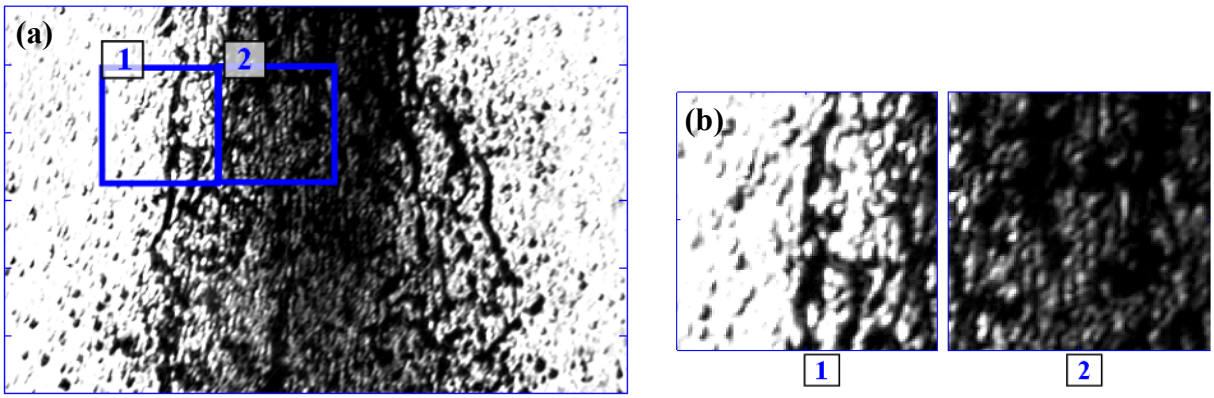

Figure 1. Example of an experimental time-gated ballistic image for an aerated water spray, 2 mm downstream from the nozzle orifice. Border tick marks indicate 1 mm image distance. Liquid structures appear as dark regions on a light background field. Magnified image regions are shown in (b).

- The *intermediate single-to-multiple scattering regime* operates when the average number of scattering events is between 2 and 9. In this regime, a single dominant scattering order is clearly defined. No approximation can be made under such a regime.

- The *multiple scattering regime* is defined when the average number of scattering events is greater or equal to 10. In this regime, the relative amount of each scattering order tends to be equal and no dominant scattering order is apparent. The diffusion approximation can be applied in this regime.

The optical depth (*OD*) can be calculated by dividing the total length, *l*, traversed by a light beam, by the mean free path length: $OD = l / \overline{l_{fp}} = l \cdot \mu_e$. The optical depth provides an estimation of the average number of times that photons have interacted with the scattering particles, prior to exiting a medium of length *l*. The classification of each scattering regime can be performed from the value of the optical depth as presented in Table 1.

Table 1. Classification of the scattering regimes as a function of the optical depth.

Single scattering regime	Intermediate scattering regime	Multiple scattering regime
$OD \leq 1$	$2 \leq OD \leq 9$	$OD \geq 10$

In the work presented here, scattering of light in the "late" intermediate and "early" multiple scattering regime is investigated both experimentally and via simulation. The focus of the article is to simulate the effect of spatial filtering and time-gating on photon selection in BI applications based on the experimental set-up described by Paciaroni [2]. Paciaroni's system was adapted from earlier work by Alfano *et al.* in the biomedical field [3-4], and was successfully applied to a Diesel spray in 2005, to image voids, and roll-up structures in the near field [5]. The present simulation models both the propagation of light through the scattering medium and transmission through the BI optics and aims to quantify the composite light filtering effects of the BI system on the spatial intensity contrast at the image plane.

Description of the simulation

The results shown here are calculated with a system model based on a Monte-Carlo (MC) solution to the radiative transfer equation (RTE) [6], integrated with a custom ray-tracing model. This scheme provides a computationally affordable approach for calculating photon scattering trajectories in regions containing a large number density of spherical droplets and allows detailed analysis of light propagation for specific flow field, source, and detection parameters. Light propagation in the model scattering volume is calculated as the sum of many distinct photon-particle interactions. Photons enter the simulated scattering medium with a defined initial position and direction of

propagation. The free path length, l, between each light-particle interaction is derived from the Beer-Lambert law and is calculated as a function of the extinction coefficient, μ_e, using a random number, ξ, uniformly distributed between 0 and 1 such that:

$$l = -\ln(\xi)/\mu_e \tag{1}$$

After a scattering event, the photon's new direction is selected based on a random number and the cumulative probability density function calculated from the appropriate scattering phase function, which is derived from Lorenz-Mie theory. When a new direction of propagation is defined, the position of the next scattering interaction is calculated and the process is repeated until the photon is either absorbed or exits the medium at a boundary. For the 800 nm laser source modeled in this work, absorption of the incident light by the scatterers is negligible, and this assumption holds for the surrounding medium as well. This chain of events is repeated for a sufficiently large number of photons such that the distribution of the light intensity impinging on the detector is accurately represented. Computed photons are recorded on the front face of the scattering volume and traced through the remaining optics to the detection plane, as shown in Figure 2. The information generated for each photon in the MC calculation is translated to ray parameters. Rays defined by the MC data are then compiled and propagated through a detailed geometric optics model of the BI instrument. The geometric optics model is constructed in Mathematica code from surface and material data for each system component, allowing low-level customization of component properties. Rays from the custom light source are traced through the model optical system by Rayica, a commercial tracing engine available as an add-on to Mathematica. The simulation presented in this work examines time-gating and spatial filtering effects on the BI signal field in the context of contrast at the image plane, where contrast is calculated from simulation test chart images, according to:

$$\text{Contrast} \equiv \frac{I_{\max} - I_{\min}}{I_{\max} + I_{\min}} \tag{2}$$

Here, $I_{\max}$ is the maximum image intensity and $I_{\min}$ is the minimum image intensity, which occurs at the centre of the bars of a test chart projected in the detection plane. The following sections present contrast results for two distinct imaging cases — a validation case based on monodisperse scattering spheres, and a case more relevant to measurements in a transient spray which assumes a polydisperse distribution of fuel droplets.

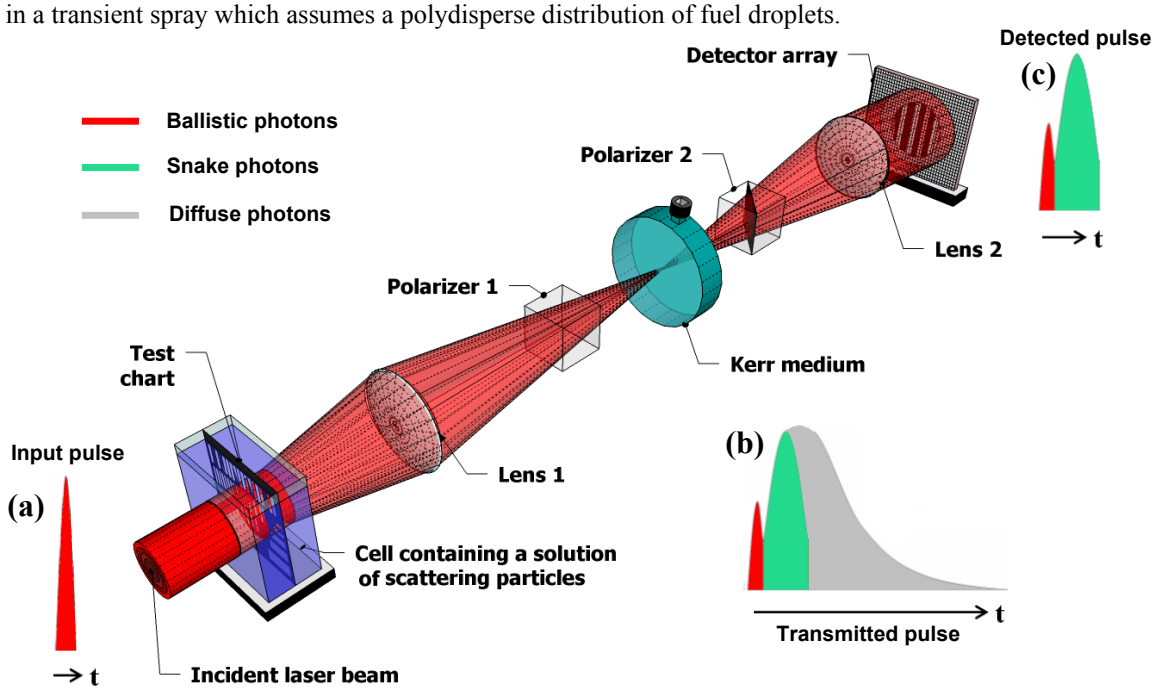

Figure 2. Simulation configuration: Photons from a 100 fs laser pulse traverse a volume (10 mm long) containing randomly distributed spherical particles with a given size distribution. Scattered light is traced through collection and time-gate optics and forms an intensity distribution at the detector. A test chart located at the center of the scattering volume (at 5 mm) allows specific spatial frequencies to be analyzed. The incident laser pulse is represented in (a); (b) is the transmitted pulse; (c) shows the portion of light reaching the detector after time gating and spatial filtering.

Case 1: Microspheres in solution

Previous work by Paciaroni [2] included careful image resolution measurements for a range of BI experimental setups using suspensions of polystyrene microspheres in water. Applying the numerical model developed for BI for the conditions used the previous experimental work allows a convenient test on the validity of the model results. In the simulation, the refractive indices of the distilled water and of the polystyrene spheres are set to 1.33 and 1.58 respectively.

Figure 3 compares simulation results side-by-side with ballistic images of a resolution test chart embedded in a volume containing a solution of polystyrene spheres, d = 0.7 μm. Figure 3 (a) and (b) show results for the detected image when the Kerr-effect shutter is not present and the entire transmitted pulse is integrated by the detector. In this case, the test pattern is barely discernible due to strong interference from multiply-scattered source light and the calculated contrast is on the order of 5%. Figures 3 (c) and (d) show results obtained when the detected light is filtered by the action of the Kerr-effect shutter. Here the detected light is gated such that late-arriving (t > 2 ps) photons are excluded from the image, resulting in dramatically improved visibility of the test pattern, and a calculated contrast on the order of 55%.

An additional benefit of the BI model is the ability to easily test parameters which are sensitive or otherwise difficult to vary in an experimental context. Figure 3(e) uses simulation results to examine the effect of time-gating on image contrast (red line) and signal intensity (blue line) for the microsphere scattering medium at optical depth, OD = 14. Note that even for such a high OD, the model shows the contrast tends to 100% when reducing the delay of the time-gate. Nevertheless, this contrast improvement comes at the cost of a severe reduction in light intensity.

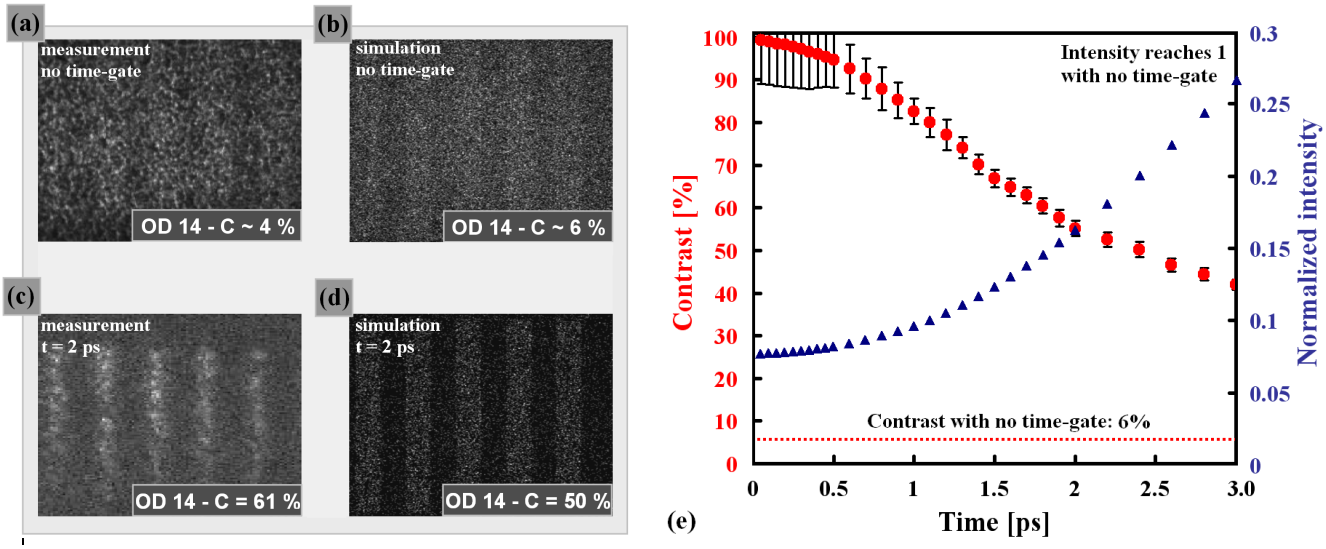

Figure 3. Simulation/measurement comparison: A resolution test chart bar pattern with a spatial frequency of 1 lp/mm is embedded in a scattering volume containing a solution of 0.7 μm spheres and imaged by the BI instrument: (a) no time-gate, (c) ~2 ps time-gating. Simulation results corresponding to experimental conditions of (a) and (c) are shown in (b) and (d). In (e) the simulation image contrast results and detected intensity are given for time-gating ranging from 0.1 to 3 ps.

Case 2: Fuel spray droplet distribution

One goal of this work is to improve diagnostics of dense multiphase flow fields such as those typical in spray applications. To this end, the numerical BI model was applied to a second set of simulations where the scattering volume contains a polydisperse Rosin-Rammler distribution of fuel droplets with a mean droplet size of 14 μm, and a representative Sauter mean diameter, d_{32} = 23 µm (Case 2).

The system model can provide specific insight into how the source light pulse spreads in space and time as it propagates through the scattering medium (10 mm long). The effect of time-gating on the image signal is straightforward if the temporal signature of the light pulse integrated at the detector is known. This signature depends strongly on the particle size and other parameters that influence the Mie-scattering phase function describing the medium, and also depends directly on the OD and dimensions of the scattering volume. Simulation results for photon arrival times are detailed in Figure 4.

Figure 4(a) compares scattering from small monodisperse particles similar to Case 1, discussed in the previous section, to the Case 2 scattering medium containing a polydisperse distribution of larger scatterers. Here, it is interesting to note that the contribution from ballistic photons is discernible for the small scatterers, but is obscured by snake photon contributions for the medium containing a range of larger particles. The change in the time-signature for scattering by the fuel droplets can be observed at $OD = 5$ and $OD = 10$ in Fig. 4(b). The contributions of the individual scattering orders are extracted in (c) for $OD = 5$ and in (d) for $OD = 10$. Note that 33.4 ps corresponds to the time for the ballistic photons to cross the 10 mm length of the probe volume in ambient air. If one neglects details of the shape of the time-gate mechanism, time-gating can be understood as simply excluding photons in the trailing edge of the broadened pulse (as illustrated in Fig.4 (a)).

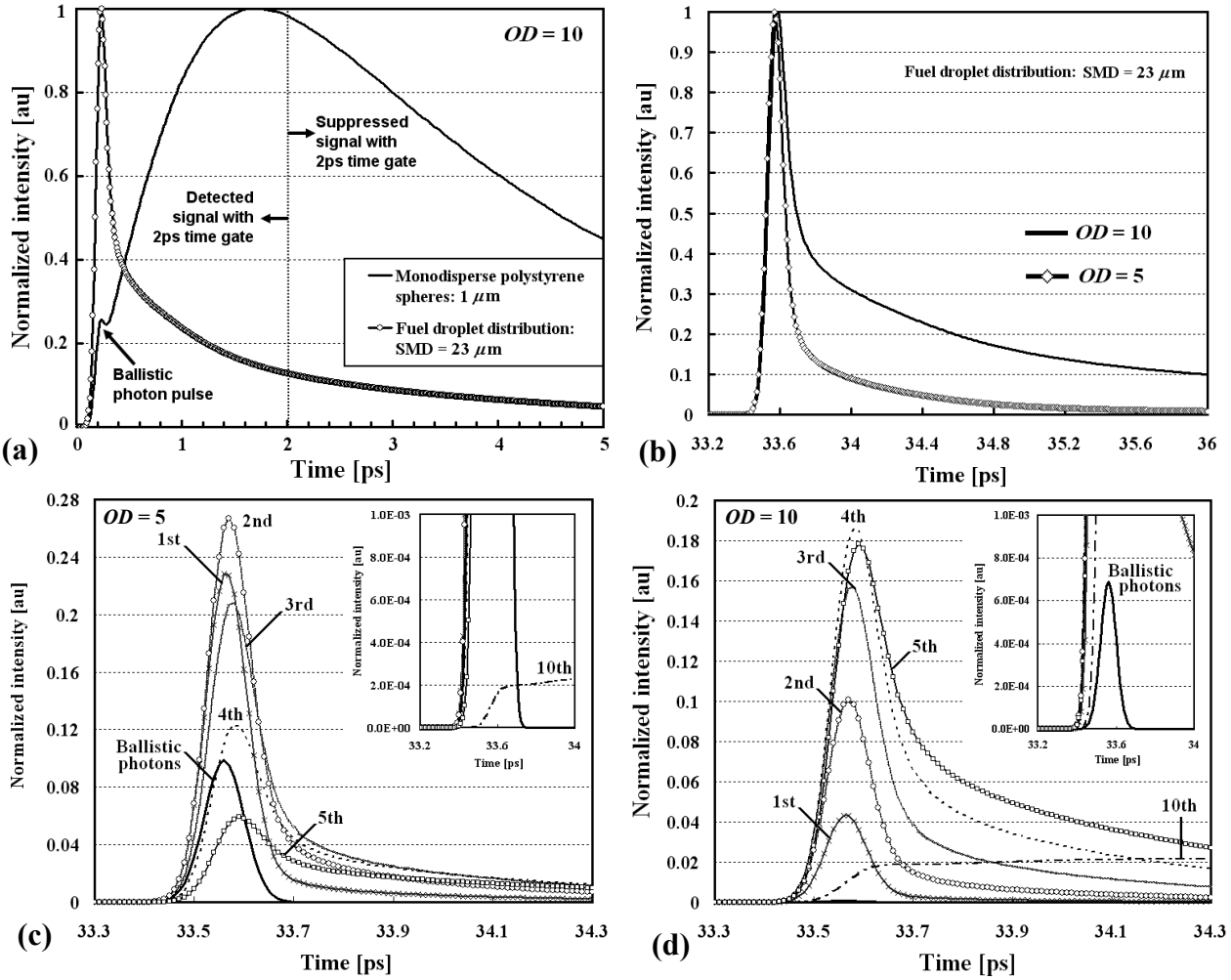

Figure 4. Time-resolved results for transmitted pulse: (a) total detected intensity for a polydisperse distribution of fuel droplets centered at 14 μm with d_{32} equal to 23 μm. Results at $OD = 10$ are compared with monodisperse scatterers of 1 μm size - (b) total detected intensity for the distribution of fuel droplets at $OD = 10$ and at $OD = 5$. The contribution of individual scattering orders is given at $OD = 5$ in (c), and at $OD = 10$ in (d).

Figure 5 shows simulation images for the Case 2 with fuel droplets at $OD = 10$. The test chart in the center of the scattering volume modulates the input light with a spatial frequency of 2 lp/mm. Figure 5 (a) corresponds to the image when no time-gating or significant spatial filtering is applied; no evidence of the resolution test chart is apparent under these conditions. This is roughly analogous to a direct shadowgram of the scattering medium. Figure 5(b) shows the same measurement volume when spatially filtered by the Kerr gate optics and time-gated at 2 ps. In this case, the overall intensity of the image is reduced, but the 2 lp/mm features of the resolution test chart are now clearly visible.

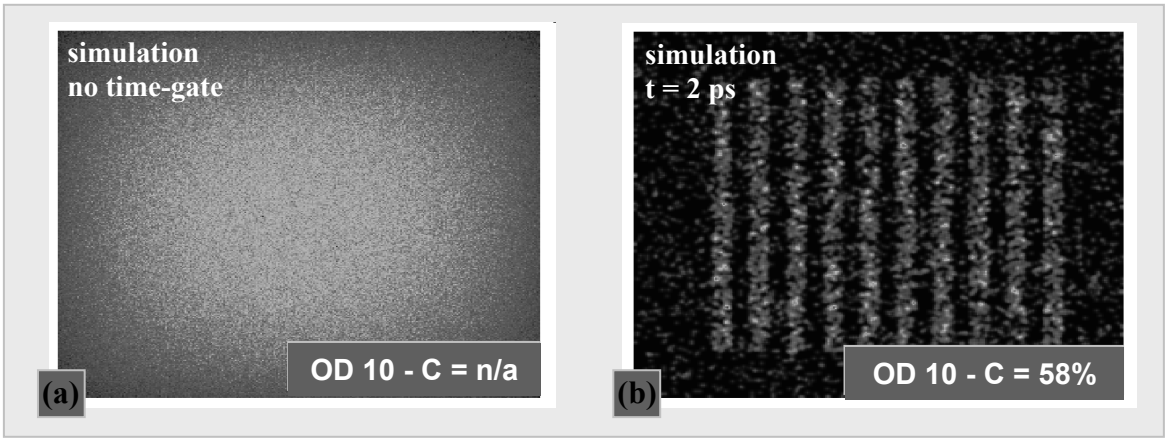

Figure 5. Simulation image results after scattering through polydisperse 14 μm fuel droplet distribution with embedded 2 lp/mm resolution test chart, *OD* = 10 (a) unfiltered image; no discernible contrast. (b) spatially filtered with Kerr gate optics, and time-gated at 2 ps; contrast = 58 %.

Conclusion

The system model presented in this work, allows exploring and characterizing the effectiveness of spatial and temporal light filtering of a BI instrument. The form of the BI instrument simulated in this work was chosen based on Paciaroni's recommendations for investigations of dense sprays. Preliminary validation results for the model were presented, and compare well with experimental results from previous work. The results shown here demonstrate that ballistic imaging can significantly improve contrast in line-of-sight integrated images under optically dense conditions, consistent with the intermediate and multiple scattering regimes. The technique is effective in mitigating noise contributions, especially for large optical depths (*OD* = 10 and higher) where signals which are completely lost with no light discrimination may be recovered using appropriate spatial and temporal filtering.

Since the light scattering properties of the measurement volume and the light selection capacity of the BI system are interdependent, the numerical BI model presented here represents an essential tool for optimizing the BI instrument to yield the best results for the specific scattering environment under investigation. Results shown for Case 1 predict that, by reducing the commonly used 2 ps time-gate by a factor of two, the contrast will increase from ~50% to ~80%. Also, a 2 ps time-gate may be less appropriate for the "low" intermediate scattering regime where *OD* ~ 3 and/or for sprays of very small dimension. In such cases, a large fraction of the diffuse light would not be segregated by the 2 ps time-gating and would reach the detector. Both of these observations motivate, then, development of a still faster optical shutter, even though increased temporal segregation comes at the cost of losses in light intensity. In addition, shorter gating allows increased suppression of diffraction artifacts (e.g. ring patterns from edges or apertures) commonly observed in imaging techniques which utilize coherent light.

Acknowledgements

Support for this work was provided by the U.S. Air Force Research Laboratory under contracts FA8655-06-13031 and FA8655-08-13019, CECOST through Swedish Statens Energimyndigheten grant no. 20437-1, and the Swedish Vetenskapsrådet under grant no. 621-2004-5504.

References

1. Linne, M., Paciaroni, M., Berrocal, E., Sedarsky, D., *Proc. Comb. Inst.,* 32:2147-2161 (2009).
2. Paciaroni, M., *Ph.D. Thesis*, Division of Engineering, Colorado School of Mines, Golden, USA (2004).
3. Yoo, K., Alfano, R., *Opt. Lett.*, 15(6):320-322 (1990).
4. Wang, L., Ho, P., Liu, F., Zhang, X., Alfano, R., *Science*, 253:769 (1991).
5. Linne, M., Paciaroni, M., Hall, T., Parker, T., *Exp. Fluids*, 40(6):836-846 (2006).
6. Berrocal, E., Sedarsky, D., Paciaroni, M., Meglinski, I., Linne, M., *Opt. Express*, 15:10649-10665.